Part II. A Portable Miniaturized Metabolic Gas Analysis System

Tammy Anderson, Joseph Orr Ph.D.

Introduction

Previously we proposed construction of a miniaturized metabolic monitor that could be taken aboard the space station to monitor the physiological response of the body in a microgravity environment. The prototype consisted of an on airway non-dispersive infrared (NDIR) CO_2 sensor and a luminescence-quenching O_2 sensor to measure gas concentrations, and differential pressure ports to measure gas flows. Our motivations, prototype design considerations, and initial experiments were presented in a previous paper.[1] This paper aims to further examine the efficacy of the prototype device through 1) characterization of the flow profile by using a discharge coefficient, and 2) validation of the oxygen sensor at the high volumetric flows.

Characterization of Flow Profile

Flow sensing devices measure gas flow based on a transducer signal that is integrated over time to produce volume. When a flat plate with a small opening is inserted into the pipe perpendicular to the flow, the restricted opening causes a pressure drop. The obstacle created by the orifice causes the fluid particles to collide with each other, converting the velocity into heat and pressure. The added pressure increases the velocity of the particles passing through the orifice opening. Once through the opening the pressure is released. Pressure taps before and after the orifice plate measure the differential pressure drop. A resistive unit within the sensor produces a signal proportional to the pressure drop. Based on a modified Bernoulli equation, the flow rate is roughly proportional to the square root of the differential pressure. While a detailed derivation is provided elsewhere, the final equation is given by

$$Q_{stp} = \frac{P_f T_{stp}}{P_{stp} T_f} C_d \sqrt{\frac{\Delta P T_f}{M_m P_f}} \qquad (1)$$

where P_f and P_{stp} represents the pressure (mmHg) of the flowing (measured) gas and at standard temperature and pressure, respectively. Similarly, T_f, and T_{stp} represents the temperature (K). The ΔP is the differential pressure (mmHg), M_m the molecular mass, and C_d is the discharge coefficient.[2]

The discharge coefficient is needed because nonlinear differential pressure sensors calculate flow indirectly so it is necessary to adjust the flow calculations to correct for head loses and turbulent flow. This correction factor is dependent on many factors including the Reynolds number, sensing tap locations, length of the orifice, and orifice diameter. Therefore, the discharge coefficient is specific to each individual sensor design as follows. [3,4]

The differential pressure was recorded across a wide range of volumetric flows and stored in a lookup table. The table, indexed by the Reynolds number, was then incorporated into the software algorithms. The accuracy of the flow measurements with the adjustment of the discharge coefficient verses the actual recorded flow are also reported.

Materials and Methods

Constant air flow at ambient conditions was provided by an ESPRIT Ventilator (Phillips-Respironics, Carlsbad, California). The ventilator was connected to the high flow input on a VT Plus Gas Flow Analyzer (Bio-Tek, Winooski, Vermont). This served the purpose of verifying the flow rate setting selected on the ventilator. The VT Plus was calibrated using a 3 liter syringe and found to be within ±1.60%. The flow sensor was connected to the high flow exhaust on the VT Plus. The sensor was connected to the FloTrac Elite and then to a

laptop. NICO Data collection software recorded the oxygen, carbon dioxide, and differential pressure signals. The average volumetric flow was recorded from 2-300 L/min.

Results

The analogue-to-digital (ADC) differential pressure signal was recorded was recorded at incremental flow rates from 0 to 300 liters/minute, the maximum volumetric flow that could be obtained with the ventilator. For discharge coefficient analysis the ADC signal was converted into SI units of pressure. Pressure and temperature of the flowing gas were measured at P_f = 84.5 kPa and T_f = 297.5 K. The molecular mass of air was defined as M_m = 0.028669 kg/mol. According to the National Institute of Standards Technology, a standard pressure of P_{stp} = 101.325 kPa and temperature of T_{stp} = 293.15 K were used in the calculations. **Equation 1** was solved for C_d using the measured volumetric flows and the given values listed above.

The flow coefficient lookup table was generated and indexed by the Reynolds number

$$\mathrm{Re} = A\sqrt{\Delta P}\frac{M_m P_f}{\mu T_f} \quad (2)$$

where μ was the dynamic viscosity (Pa s) and A was a constant term which includes the diameter of the breathing circuit, the gas compressibility factor and the universal gas constant. The nature of the prototype was such that a specific diameter of the breathing circuit was not defined. Instead, the constant was set equal to one. Hence, the reported Reynolds number reported was scaled. This was denoted by the prime symbol following the Reynolds number, R'.

Figure 1 shows the raw flow coefficient values across the range of the Reynolds number. During laminar flow (low Reynolds numbers) there was a sharp spike seen in the flow coefficient. As the Reynolds number increases the flow coefficient stabilized around 30.5.

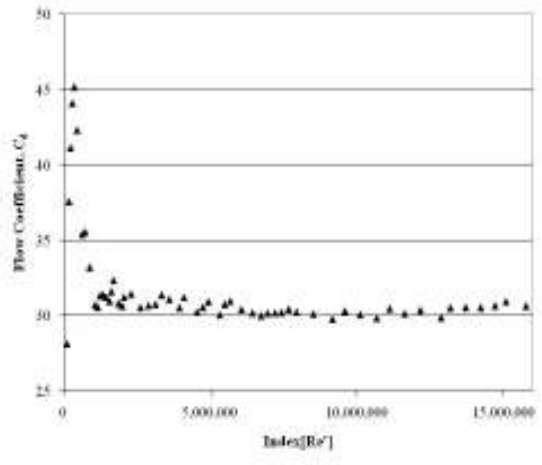

Figure 1 The discharge coefficient C_d indexed by a scaled Reynolds number

For the index table that would be incorporated into the flow algorithms the flow coefficient values were weighted. The measured volumetric flow was more dependent on the flow coefficient at low Reynolds numbers than at high ones. For an R' < 2,300,000, an average of ±1 data point to the right and the left of the flow coefficient was taken, for a total of n = 3 data points. Above R' >= 2,300,000 the flow coefficient remained stable and was set at a constant value of 30.4822.

The index table is given in **Table 1**. For values not specified on the table, a linear interpolation between the two nearest integers should be applied.

Table 1 The discharge coefficient table indexed by a scaled Reynolds number

R'	C_d	R'	C_d
111804	28.1311	1234175	31.0938
172569	35.6126	1334371	31.3202
232476	40.9369	1438328	31.1962
288890	43.4748	1559968	31.2520
358718	43.8701	1624618	31.3012
454960	40.9708	1696356	31.2526
625447	37.2761	1869371	30.9505
731142	34.2370	1989604	30.8983
884307	32.6726	2055320	31.1084
1065856	31.4932	>2300000	30.4822
1155241	30.8690		

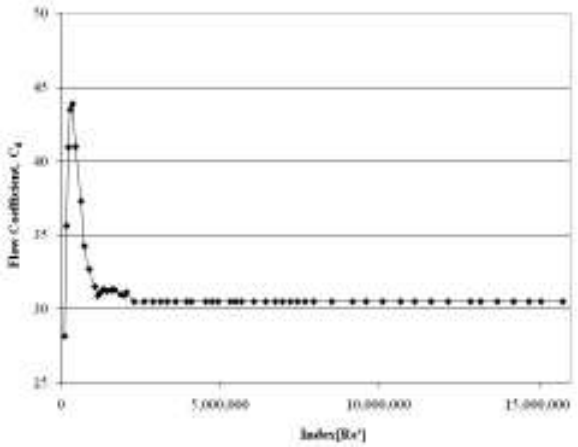

Figure 2 The weighted discharge coefficient as it would be referred to in the software algorithms

Figure 2 is a graphical representation of the weighted flow coefficients. To test the accuracy of the sensor using the modified discharge coefficient, the calculated volumetric flow was compared to the recorded volumetric flow. For an R>=650,000 to be within 3%; for R<650,000 the sensor was accurate to within ±0.8 liter.

Discussion

Orifice plates are commonly used to measure the flow of natural gases. The need for a discharge coefficient to account for head losses and changes in area that cannot be calculated theoretically has been recognized. When the orifice opening is circular, guidelines set forth by the International Organization of Standards (ISO) detail the process for determining the discharge coefficient based on empirical equations (ISO 5167-1).[5,6]

Theoretically the flow rate could also be calculated experimentally using the equation

$$Q = Av \quad (3)$$

where Q is the volumetric flow, *v* is the velocity, and A is the area of the orifice. However, the geometry of the orifice opening is not easily calculated because the orifice contains a conduit for the drainage of saliva and moisture. Moisture buildup along the inner wall of the sensor around the orifice ring can effectively change the sensor geometry.

The Reynolds number is a dimensional number that was used as a way to quantify the effects of the inertial and viscous forces within a fluid. When the predominant forces are viscosity, the fluid profiles are streamline. This is known as laminar flow and is characterized by a constant fluid motion, minimal disruptions, and a Reynolds number less than 2,300. When the Reynolds number is above 2,300 the flow is turbulent. The inertial forces become more prevalent and the flow experiences random eddies and other disturbances. Because the Reynolds number in this study was scaled, the transition from laminar to turbulent flow does not occur at R=2,300.

The flow coefficient for the prototype sensor revealed a sharp spike at low flows, followed by a transition period, and then the flow coefficient stabilized. This pattern was observed in several independent trials. In their studies of small sharp-edged cylindrical orifices, Ramamurthi et al (1999) found that at low Reynolds numbers the flow profile varied based on the aspect ratio of the length to the diameter of the orifice (*l/d*). They suspect the spike in discharge coefficient could be a result of added pressure due to the surface tension of water. When the Reynolds number is high, the surface tension induced pressures are negligible. The discharge coefficient is no longer dependent on the flow profile (i.e., Reynolds number).[7-9]

As seen in the derivation, the flow coefficient is highly sensitive to changes in the geometry of the orifice and flow profiles. One limitation of this study was the flow sensor calibration was based on a single prototype system. Before the system could be sold commercially several prototype systems with the exact same specifications would be manufactured. To improve the accuracy of the flow coefficient, each individual system could be calibrated and the results reported as a composite flow coefficient table.

Another limitation of the experimental design was the sensor was tested under

constant airflow. During a practical application, the sensor will be subjected to various expired flow rates as the individual breaths in and out. At low flows the resolution of the signal decreases, but at high flows the signal strength is high. During a normal breath this could be problematic since the flow during the exhale breath is drawn out. However, during exercise the transition of flow from an inhale to and exhale happens rapidly and there is a minimal amount of time spent while flow is low.

Validation of Oxygen Sensor

In vitro testing of oxygen uptake during exercise was performed using a propane combustion patient lung simulator. The ratio of the rate of carbon dioxide production per minute (VCO_2) over the rate of oxygen consumption per minute (VO_2) is known as the respiratory quotient (RQ). When burned completely, the combustion of propane to form carbon dioxide and water vapor has a standard RQ of 0.6. This method is often used to check the accuracy of VO_2 and VCO_2 measurements for metabolic monitors.[10,11]

In previous bench testing of the oxygen uptake measurements for clinical use, the oxygen sensor was found to be accurate to within 0.3±2.8% of the measured oxygen. When compared with the clinical gold standard device (Deltatrac, Datex, Helsinki, Finland) the error in the oxygen consumption of 2.2±4.1% was found to be well within an acceptable range for clinical use. The system was again tested on 14 intensive care unit patients and found to be within 1.7±6.9% of the reference analyzer.[12-14]

Oxygen consumption was determined theoretically and then compared to the measurements recorded during the propane simulation with constant air flow. To be suitable for an exercise application, the oxygen sensor measurement should be accurate to within ±5% of the measured fraction of expired oxygen.

Experimental Design

A propane burner was mounted inside a glass chamber with inlet and outlet flows. The inlet flow was connected to an ESRIT Ventilator (Phillips-Respironics, Carlsbad, California), which provided the oxygen necessary for combustion. The rate of inspired air V_I (L/min) was measured using the VT Plus Gas Flow Analyzer (Bio-Tek, Winooski, Vermont) before it entered the chamber. The differential pressure and oxygen sensors provided on-airway analysis of the gas as it exited the chamber in the outlet flow.

The burner was connected to a flow rotometer with a needle valve (NV). The arbitrary settings on the needle valve controlled the propane flow rate. A calibration curve was generated to relate the NV setting and hence propane combustion (by loss of mass) to the oxygen consumption. To keep the system cool and prevent damage to the parts, cold water was circulated in coils within the glass chamber.

The oxygen and differential pressure sensors were connected to a FloTrac Elite (Phillips-Respironics, Carlsbad, California), which used algorithms to determine the fraction of expired oxygen and gas flow. The FloTrac Elite was connected to a laptop, which recorded the various parameters including fraction of expired carbon dioxide ($FeCO_2$), the fraction of expired oxygen (FeO_2), and flow signals.

The accuracy of the oxygen sensor was tested at four propane combustions levels, which corresponded to the needle valve placement at 15, 20, 25 and 30. At ambient conditions, the VO_2 at these levels was determined in the calibration to be approximately 323, 430, 538, and 646 ml/min, respectively.

The same NV and flow rate settings were used for the O_2 sensor validation as in the calibration curve. A stabilization period of 5 minutes was allowed in between each NV setting. Then the V_I, FeO_2, $FeCO_2$, and differential pressure were all recorded every 3 minutes for 9 minutes total at each flow increment and the average was reported. Relative humidity and temperature of the inspired and expired gas were monitored using

an Omega RH81 Thermo Hydrometer (Omega, Stamford, Connecticut).

Relative Humidity Correction

Dry air is a composite of 78.8% nitrogen, 20.9% oxygen, 0.9% argon, and 0.03% carbon dioxide. However, for most practical applications there is also 1-3% water vapor present, so it was necessary to adjust the composition percentages of the inspired gases accordingly. For the calculations it was assumed that the fraction of inspired argon and carbon dioxide were negligible.

Analysis of Calculated FeO_2

The rate of oxygen consumption (VO_2) is the difference between the volumes of inspired air (V_I) multiplied by the fraction of inspired oxygen (F_IO_2) and the volume of expired air (V_E) multiplied by the fraction of expired oxygen (F_eO_2) as shown

$$\dot{V}O_2 = \left(\dot{V}_I * F_I O_2\right) - \left(\dot{V}_E * F_E O_2\right) \quad (4)$$

N_2 is neither used nor produced in metabolism. Therefore, the volume of N_2 inhaled must be equal to the volume exhaled according to the Haldane transformation as follows

$$\dot{V}_I \times F_I N_2 = \dot{V}_E \times F_I N_2 \quad (5)$$

where

$$F_I N_2 = 1 - F_I O_2 - F_I CO_2 - F_I H_2 O \quad (6)$$

and

$$F_E N_2 = 1 - F_E O_2 - F_E CO_2 - F_E H_2 O \quad (7)$$

Assuming that there was minimal carbon dioxide in the air (i.e. F_ICO_2 = 0) the equation yields

$$\dot{V}_E = \dot{V}_I \frac{F_{I N_2}}{F_{EN_2}} = \left(\frac{\left(1 - F_I O_2 - F_I CO_2 - F_I H_2 O\right)}{\left(1 - F_E O_2 - F_E CO_2 - F_E H_2 O\right)} \right) \dot{V}_I \quad (8)$$

Where the known parameters included V_I, which was recorded by the VT Plus; VO_2, which was calculated from the calibration curve; and FiO_2, FiH_20, $FeCO_2$, and FeH_20, which were adjusted based on the relative humidity at ambient conditions. It was a straightforward process to isolate and solve for the calculated value of FeO_2.

Results

The results of the calibration curve are shown in **Table 2.** The total mass loss from the propane combustion at each needle valve setting is shown in the first column. The molecular weight of propane was used to calculate the number of moles burned. Using the ambient conditions and the ideal gas law, the volume in ml/min of oxygen at each needle valve setting was determined in column four. At standard conditions one mole of gas occupies 22.4 liters, as shown in the last column. At ambient conditions, the volume of oxygen consumed (ml/min) was equivalent to 21.544 (R^2=0.9998) times the needle valve placement.

Oxygen Validation and Percent Error

At the ambient conditions measured in the lab, the temperature and relative humidity of the inspired air were T = 304.5 K and a RH = 23.1%. The barometric pressure was recorded at P_{bar} = 635 mm Hg. When adjusted for the relative humidity, the fractions of inspired air are as follows FiO_2 = 0.206602, $FiCO_2$ = 0, and FiH_2O = 0.012891.

The recorded FeO_2 by the oxygen sensor is given in **Table 3.** Two data points are marked with an asterisk. At 10 L/min and a NV = 30 the flame would not stay lit and no measured parameters were reported. This was

Table 2 Calibration Curve Conversion

NV	C_3H_8 g/min	C_3H_8 mol/min	5 VO_2 mol/min	VO_2 STP ml/min
15	0.0952	0.0022	0.0108	241.7565
20	0.1269	0.0029	0.0144	322.3420
25	0.1587	0.0036	0.0180	402.9274
30	0.1904	0.0043	0.0216	483.5129

Table 3 Recorded FeO_2 by the luminescence-quenching O_2 sensor

NV	10 L/min	15 L/min	25 L/min	40 L/min	60 L/min
15	17.53	18.57	19.46	19.98	20.07**
20	16.77	18.12	19.03	19.84	20.15
25	16.03	17.65	18.91	19.73	20.11
30	*	17.21	18.65	19.60	19.95

* Flame would not stay lit at this flow
** Flow did not reach 60 L/min

Table 4 The percent error between the calculated FeO_2 and the recorded FeO_2

NV	10 L/min	15 L/min	25 L/min	40 L/min	60 L/min
15	1.44%	0.87%	0.87%	0.61%	0.26%**
20	2.81%	2.18%	0.93%	1.54%	1.20%
25	5.77%	3.47%	2.45%	2.19%	2.05%
30	*	5.13%	3.78%	3.32%	2.57%

* Flame would not stay lit at this flow
** Flow did not reach 60 L/min

most likely caused by the large propane consumption being limited by available oxygen in the low flow. At 60 L/min and a NV = 15 the V_I is lower than at the other flows (~50 L/min instead of ~60 L/min). Although the FiO_2 and percent error are reported for this value, it is important to take the decrease in V_I into consideration.

From the calibration curve, the VO_2 at each needle valve setting (which relates to the flow of propane controlled by the rotometer) was determined. Going down the columns for a given flow rate, the FeO_2 measured in the output flow decreased with increasing propane combustion rates (higher NV settings) and VO_2. Moving across the rows, when the propane combustion is held constant the FeO_2 increases with increasing flow rates. The difference in FeO_2 between the NV settings is more pronounced at lower flows. As the flow increases the difference becomes less significant.

The theoretical FeO2 was calculated. A comparison of the theoretical FeO_2 and the FeO_2 recorded by the oxygen sensor is given in **Table 4.** The percent of error was greatest at the low flows and decreased as the flow increased for a given propane level. At constant flow the percent error increased as the propane consumed also increased. As previously noted, the flow at NV = 15 and 60 L/min was lower than the others. While the exact FeO_2 could not be measured, the trend remained consistent.

The chamber design required cooling coils to remove heat within the chamber. Circulating water was pumped the water through the coils. Ice was occasionally added to the water to keep the water at 29° C. This had the immediate effect of reducing the relative humidity in the expired gas, and could possibly why the percent error at NV = 20 and 25 L/min (**Table 4**) was slightly lower than expected even though the recorded FeO_2 (**Table 3**) at that point was within the expected range.

Discussion

The *in vitro* simulation of an exercising individual conducted in a propane burn combustion chamber found the luminescence quenching oxygen sensor to be accurate within ±6% of the expected FeO_2 at the ambient conditions across the entire range of flows tested. The accuracy of the sensor improved as the flow rates increased.

The experimental design had a few limitations. First, the simulation of exercise was limited by the size of propane combustion chamber. Flows larger than 60 L/min would extinguish the flame. During maximal exercise, the minute ventilation of an average 40 year old male is about 90 L/min. Athletes at their peak have minute ventilations that can exceed 200 L/min. This chamber size is more representative of the minute volumes a child would require during exercise.

Another limitation related to the chamber size was the allowable flame size for the propane combustion. During exercise, a 40 year old male weighing 75 kg may have a VO_2 max of 40 ml/kg/min or 3000 ml/min. The flame size limited the maximum oxygen consumption to about 640 ml/min. So even

though the sensor is accurate to within ±3% at the highest flow rate and VO_2 consumption level tested, the accuracy of the oxygen sensor at higher VO_2 levels and flow rates could not be determined.

Relative humidity can also cause errors in the reported oxygen consumption. Relative humidity of the expired gas was measured and the gas analysis was adjusted accordingly. At low air flow rates the expired gas was nearly 100% saturated. However, as the flow rate increased the water concentration in the expired air was diluted. The relative humidity at 60 L/min was around 25%. Air exhaled from the lungs becomes saturated, so this limitation in the experimental design must also be considered.

The most significant limitation was most likely caused by a span error due to the calibration of the oxygen sensor performed by the black box. Span is the variation from the input oxygen and the output oxygen signal. The oxygen sensor was calibrated by zeroing the sensor in room air. The expired oxygen signals that were closest to the inspired oxygen signals had lower error than expired oxygen that was farther away from the original value. To reduce the span error the sensor should be zeroed in an additional gas like nitrogen.

Despite the limitations, the purpose of these experiments was to determine if the luminescence-quenching oxygen sensor designed for low flow applications could be expanded to include elevated volumetric air flows. During exercise both flow rates and oxygen consumption levels increase, so it is reasonable to conclude that the FeO_2 measured would still be within the limits of sensitivity for the oxygen sensor.

Conclusions

The overall goal was to determine if modifying an existing metabolic system for exercise testing was reasonable. Based on the results presented in Part I and Part II and notwithstanding the limitations, we concluded that the performance of the prototype system indicates it would indeed be possible to build such a system. The system applications could extend to several large markets and would be profitable.

References

1. Anderson T, Orr, Joe: A Prototype Miniaturized Metabolic Gas Analysis System, Rocky Mountain NASA Space Grant Consortium. Logan, Utah, 2010
2. Anderson T: Feasibility Study of a Prototype Miniaturized Metabolic Gas Analysis System for Maximal Exercise Testing, Bioengineering. Salt Lake City University of Utah 2010, pp 90
3. Page RT: Constant-Flow Orifice Meters of Low Capacity. Industrial & Engineering Chemistry Analytical Edition 1935; 7: 355-358
4. Keyser D, R., Jeffrey, R. Friedman: Extrapolation and Curve-Fitting of Calibration Data for Differential Pressure Flow Meters. Journal of Engineering for Gas Turbines and Power 2010; 132: 024501
5. Measurement of fluid flow by means of pressure differential devices, Part 1: Orifice plates, nozzels, and Venturi tubes inserted in circular cross-section conduits running full. , International Organization of Standards, 1991
6. Reader-Harris MJ, Sattary JA: The orifice plate discharge coefficient equation. Flow Measurement and Instrumentation 1990; 1: 67-76
7. Laws EM, Ouazanne AK: Compact installations for differential flowmeters. Flow Measurement and Instrumentation 1994; 5: 79-85
8. Reed SB, Sprange MP: Flowmeter Calibrated for Any Gas in the Range of 1 to 500 Liters per Hour. Industrial & Engineering Chemistry Fundamentals 1968; 7: 651-655
9. Johansen FC: Flow through Pipe Orifices at Low Reynolds Numbers. Proceedings of the Royal Society of London. Series A, Containing Papers of a Mathematical and Physical Character 1930; 126: 231-245
10. Weissman C, Sardar A, Kemper M: In Vitro Evaluation of a Compact Metabolic Measurement Instrument. Journal of Parenteral and Enteral Nutrition 1990; 14: 216-221
11. Melendez JA, Veronesi M, Barrera R, Ferri E, Miodownik S: Determination of metabolic monitor errors and precision under clinical conditions. Clinical Nutrition 2001; 20: 547-551
12. Orr J, Brewer, Lara: Oxygen Uptake (VO2) Measurement System Based on Novel Luminescence-Quenching On-Airway Oxygen Sensor. Anesthesiology 2007; A1642
13. Orr J, Brewer, Lara: Evaluation in Volunteers of a VO2 Measurement System Based on a Novel On-Airway Oxygen Sensor Anesthesiology 2008; A1689
14. Orr J, Brewer, Lara: Clinical Evaluation of an On-Airway System to Measure Oxygen Uptake. . Anesthesiology 2008; A281